Journal of Power Sources 195 (2010) 2029–2035

Contents lists available at ScienceDirect

Journal of Power Sources

journal homepage: www.elsevier.com/locate/jpowsour

Cycling and rate performance of Li–$LiFePO_4$ cells in mixed FSI–TFSI room temperature ionic liquids

A.P. Lewandowski [a,b], A.F. Hollenkamp [b,*], S.W. Donne [a], A.S. Best [b]

[a] Discipline of Chemistry, University of Newcastle, Callaghan, NSW 2308, Australia
[b] CSIRO Division of Energy Technology, Bayview Avenue, Clayton, VIC 3168, Australia

ARTICLE INFO

Article history:
Received 7 August 2009
Received in revised form
17 September 2009
Accepted 12 October 2009
Available online 30 October 2009

Keywords:
Lithium
Battery
Lithium iron phosphate
Ionic liquid
Pyrrolidinium
Specific capacitance

ABSTRACT

A study is conducted of the performance of lithium iron(II) phosphate, $LiFePO_4$, as a cathode material in a lithium secondary battery that features an ionic liquid electrolyte solution and a metallic lithium anode. The electrolyte solution comprises an ionic liquid of a N-methyl-N-alkyl-pyrrolidinium (alkyl = n-propyl or n-butyl) cation and either the bis(fluorosulfonyl)imide $[(FSO_2)_2N^-]$ or bis(trifluoromethanesulfonyl)imide $[(F_3CSO_2)_2N^-]$ anion, together with 0.5 mol kg^{-1} of lithium bis(trifluoromethanesulfonyl)imide salt. For N-methyl-N-propyl-pyrrolidinium bis(fluorosulfonyl)imide, coin cells discharging at rates of C/10 and 4C yield specific capacities of 153 and 110 mAh g^{-1}, respectively, at an average coulombic efficiency of 99.8%. This performance is maintained for over 400 cycles at 50 °C and therefore indicates that these electrolyte solutions support long-term cycling of both $LiFePO_4$ and metallic lithium while, due to the negligible volatility of ionic liquids, surrounding the lithium in an inherently safe, non-flammable medium.

1. Introduction

The demand for rechargeable batteries with longer cycle-lives and higher performance for modern electrical devices continues to increase. For many years, these needs have been met by variants of the lithium-ion battery that was first commercialized by Sony [1]. While this technology has been refined to different degrees, the battery is still essentially composed of: (i) a layered metal oxide cathode material in which charge-transfer associated with redox reactions is balanced by lithium-ion (de)intercalation; (ii) a graphite-based anode which is able to host lithium in its reduced form; (iii) an organic electrolyte solution that incorporates a lithium salt (e.g., $LiPF_6$). The best-performing layered metal oxides contain cobalt, which is relatively costly and of limited supply [2,3]. In addition, ultimate stability (cycle-life) of these materials is questionable as it has been shown that cobalt can be leached by the electrolyte solution [4]. Issues such as these have driven the research into a range of other cathode materials.

Since first proposed by Padhi et al. [5] in 1997, $LiFePO_4$ has attracted much interest and has been well considered as the next-generation cathode material for commercial secondary lithium batteries. As illustrated in Fig. 1, $LiFePO_4$ has an orthorhombic olivine structure which consists of $[FeO_6]$ octahedra with oxygen corner-sharing $[PO_4^{3-}]$ tetrahedra (space group: Pnma). With a high theoretical capacity (170 mAh g^{-1}), which compares well with previously used $LiCoO_2$ (140 mAh g^{-1}), $LiFePO_4$ is environmentally friendly (low toxicity) and occurs naturally as the mineral triphylite [6]. The typical discharge potential of 3.45 V vs. Li/Li^+ is reasonably close to corresponding values for many layered metal oxides. The major perceived problem with $LiFePO_4$ is its low electrical conductivity [7] which, combined with low lithium diffusion at the interface [5], leads to limited charge–discharge rate capability [8]. Improved conductivity has been achieved with the development of synthetic methods that leave $LiFePO_4$ particles carbon-coated, thereby raising typical conductivity values from ca. 10^{-9} to 10^{-4} Scm^{-1} [9].

The use of metallic lithium anodes has long been recognized as a way of greatly increasing the specific energy of cells [10], which is limited for carbon host materials to a theoretical maximum of 372 mAh g^{-1}. More recently developed host materials (e.g., SnO and Si [11]) offer increased energy performance but questions remain over long-term stability due to large differences in the volume between charged and discharged states. Unfortunately, the shape of a lithium metal electrode is difficult to control as the charging (deposition) phase tends to produce branched (dendritic) morphologies which eventually form short-circuits [12]. The dendritic initially cause a loss of charging efficiency, and then become centres of internal heating. The standard electrolyte solutions, based

* Corresponding author at: CSIRO Division of Energy Technology, Energy Storage Technologies, Gate 1, Bayview Avenue, Clayton, VIC 3168, Australia.
Tel.: +61 0 3 9545 8500.
E-mail address: tony.hollenkamp@csiro.au (A.F. Hollenkamp).

0378-7753/$ – see front matter.
doi:10.1016/j.jpowsour.2009.10.059

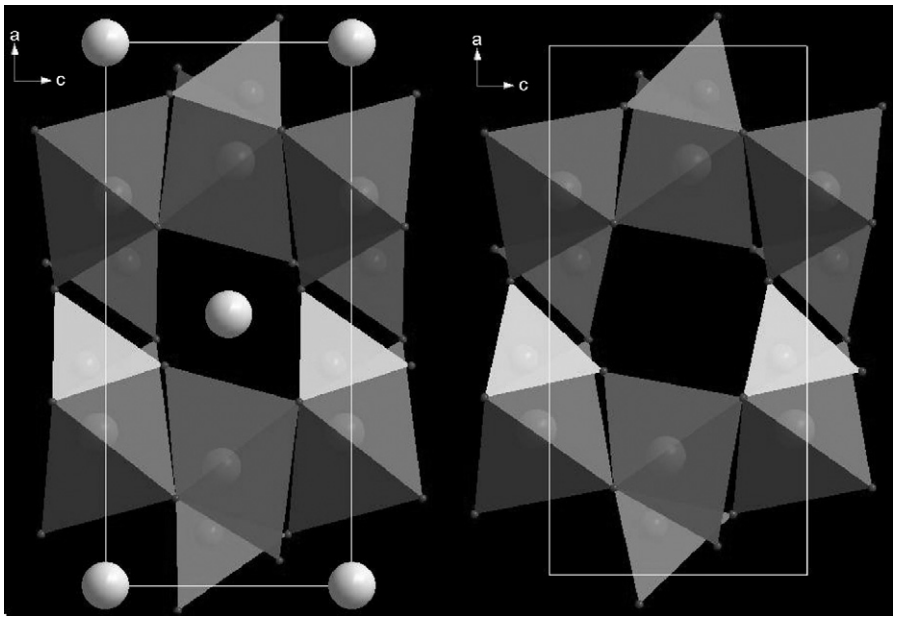

Fig. 1. Crystal structure of LFP (left) and FP (right) in (0 1 0) direction. Spheres, tetrahedra and octahedra denote lithium ions, (PO_4^{3-}), and (FeO_6), respectively.

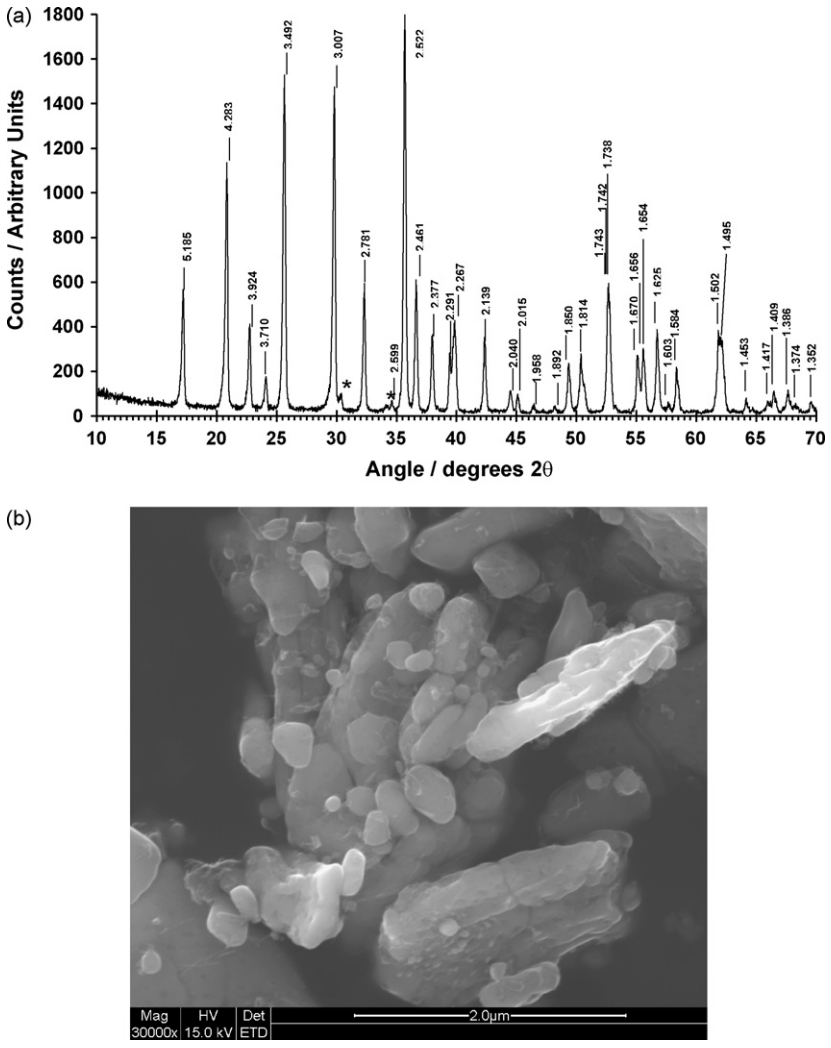

Fig. 2. (a). X-ray powder diffraction pattern of $LiFePO_4$. *Indicates residual $Fe_4(P_2O_7)_3$ precursor [27]. (b) SEM image of $LiFePO_4$ powder particles.

on mixtures of organic carbonates and ethers (with $LiPF_6$) ultimately boil and create a situation where explosive venting of the battery may occur, probably accompanied by fire [13–16]. With carbonaceous anode materials, though, these solutions form a stable solid electrolyte interphase (SEI) through which lithium ions can diffuse at very high rates. Carbonate-based electrolytes also combine excellent liquid properties with sufficient oxidative stability [17–20].

Within the last few years it has been shown that lithium-bearing electrolyte solutions based on room temperature ionic liquids (RTILs) can support highly reversible deposition and stripping of lithium. For example, Howlett et al. [21] cycled lithium electrodes efficiently in N-butyl-N-methyl-pyrrolidinium bis(trifluoromethanesulfonyl)imide (C_4mpyrTFSI) (with 0.5 mol kg^{-1} LiTFSI), with no sign of dendrites, at rates up to 1.0 A cm^{-2}. It was subsequently suggested that the SEI that forms in this system is protective as well as being highly conductive to lithium ions [22]. RTIL-based electrolyte solutions have the advantage of negligible volatility and this virtually removes the danger of explosion and fire [2]. They also offer reasonable conductivity and a wide liquid range [23]. Several groups have also investigated the interaction of RTIL-based electrolyte solutions with lithium-intercalating cathode materials [13,14,24,25]. While layered oxides such as $LiCoO_2$ do not seem to be stable with respect to metal leaching, $LiFePO_4$ appears compatible with RTIL electrolytes. Interestingly, some early trials of carbonaceous anode materials with imidazolium TFSI ionic liquids revealed rapid loss of performance [26]. Improved performance has been found recently by replacing TFSI with its lighter homologue, FSI [bis(fluorosulfonyl)imide] [2].

In this study, an attempt is made to combine the safety and cycle-ability of a lithium-bearing pyrrolidinium ionic liquid electrolyte solution with a $LiFePO_4$ cathode and a metallic lithium anode of high specific energy to produce a safe, high-performance rechargeable lithium battery.

2. Experimental

2.1. Materials

Lithium iron(II) phosphate ($LiFePO_4$) with 1.7 wt% carbon was obtained from Phostech Lithium (Quebec, Canada). The ionic liquid C_4mpyrTFSI was obtained from Merck and was dried at 45 °C for 2 days, while N-propyl-N-methyl-pyrrolidinium bis(fluorosulfonyl)imide (C_3mpyrFSI) was obtained from Dai-Ichi Kogyo Seiyaku Co Ltd. (Kyoto, Japan) and was used as-received. LiTFSI was obtained from 3 M Corporation and was dried at 200 °C under vacuum for 2 days. Solutions of $LiPF_6$ (1 M) in 1:1 ethylene carbonate:dimethyl carbonate (EC:DMC) were obtained from Mitsubishi Chemicals. All electrolyte materials were stored in an argon-filled glove-box. Karl Fischer titration was used to determine the water content of the neat RTILs with all samples yielding values in the range of 20–50 ppm. Solutions of LiTFSI (0.5 mol kg^{-1}) in either C_4mpyrTFSI or C_3mpyrFSI were prepared and stored in a glove-box prior to usage.

2.2. Electrode preparation

$LiFePO_4$ (75%), Shawinigan carbon black (15%) and polyvinylidene difluoride (PVdF) binder (10%) were combined in a glass jar, then thoroughly mixed by adding alumina spheres and sealing tightly and slowly rotating the jar for several hours. Afterwards, N-methyl-pyrrolidone (NMP) solvent was added until the resultant slurry had a free-flowing texture for easy pasting on to an aluminium (30 μm thick) substrate with a graded roller (60 μm grating). The pasted slurry was then left to dry under a fume hood overnight before being vacuum dried at 100 °C for several days. This led to an average active material loading density of 1.80 mg cm^{-2}.

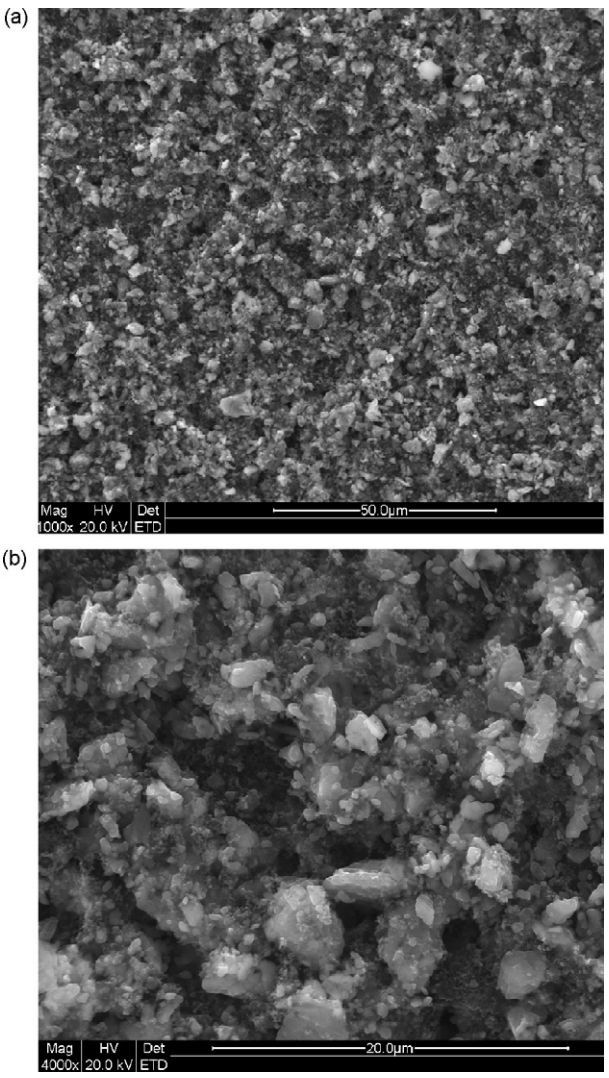

Fig. 3. Typical SEM images of surface of cathode coating ($LiFePO_4$, Shawinigan carbon black, and PVDF binder).

2.3. Electrochemical cell construction and testing

Device testing was conducted in CR2032-type cells which, in addition to the $LiFePO_4$ cathode (*v.s.*), contained a metallic lithium anode, a Solupor separator, and an electrolyte solution (based on either EC:DMC or RTIL). These cells were assembled in an argon-filled glove-box at ambient temperature. Charge–discharge experiments were performed with a Maccor Series 4000 battery cycler between voltage limits of 3.0 and 3.8 V, at various rates.

2.4. Structure and morphology characterization

The surface morphology of the $LiFePO_4$ powder and cathode samples was examined by means of scanning electron microscopy (SEM) with a FEI Quanta 400 instrument, while powder X-ray diffraction (XRD) analysis was conducted with a PANAlytical XPert PRO.

3. Results and discussion

3.1. Structure and morphology

Analysis of powder diffraction data for the $LiFePO_4$ used in this study (Fig. 2(a)) suggests that this material is well crystallized. Small peaks at $2\theta = \sim 30^\circ$ and 34° (asterisk in Fig. 2(a)) indicate the presence of residual $Fe_4(P_2O_7)_3$ precursor [27]. A typical SEM image (Fig. 2(b)) shows sub-micron particles with a size between 100 and 500 nm, as well as larger fragments, typically 1–5 μm in size. SEM images of a typical coating (Fig. 3) show a very uneven surface and, overall, a porous agglomerate structure with the smaller crystallites bound on the surface of larger ones. This would allow for more effective diffusion of electrolyte solution into the 30–40 μm thick coating shown in the images.

3.2. Electrochemical performance of Li|C_3mpyrFSI (0.5 m LiTFSI)|$LiFePO_4$ cells

A typical set of charge–discharge curves for the cell is presented in Fig. 4. Both traces feature an almost constant voltage at intermediate states-of-charge, which is a well-known characteristic of cells that incorporate this cathode material. The sharp rise and fall in voltage near the ends of the charge–discharge cycle signals the limits of lithium extraction/insertion, and that there is no prospect for significantly increasing capacity through expanding the lower and upper voltage limits. Other groups have, however, attempted to increase capacity in this way. Wang et al. [17] and Franger et al. [28] raised the upper voltage limit to 4.2 V (and above) for their studies in EC:DMC electrolyte solutions. Prosini et al. [29] and Franger et al. [18] also lowered the end-of-discharge voltage limit down to 2.0 V. In no case did the change in voltage produce a sustained increase in discharge capacity.

The discharge performance of Li–$LiFePO_4$ cells in the FSI ionic liquid electrolyte solution, for charging and discharging at the C/10 rate at 50 °C, is shown in Fig. 5(a). Discharge capacity remains steady at close to 155 mAh g^{-1} (referred to the mass of cathode active material) for the 40 cycles shown. Importantly, the charging efficiency of this cell quickly reaches a relatively high value (0.998) within 20 cycles. The cell that was prepared with conventional electrolyte also registers good cycling performance, with a discharge capacity and charging efficiency that are both close to (though slightly below) the respective values for the C_3mpyrFSI-LiTFSI cell (Fig. 5(b)). For further comparison, cell behaviour was also assessed with an all-TFSI electrolyte solution, namely, C_4mpyrTFSI with 0.5 mol kg^{-1} LiTFSI (Fig. 5(c)). In this case, the capacity reaches a much lower maximum value (just under 120 mAh g^{-1}) before commencing a steady decline. As noted by Saint et al. [30], who conducted a similar comparison, but with a series of manganese oxide cathode materials, the presence of a substantial fraction of the FSI anion appreciably lowers the viscosity of the electrolyte solution. Therefore, it is suggested here that the C_4mpyrTFSI–LiTFSI electrolyte, with the highest viscosity of the three electrolytes, actually does not fully penetrate the cathode pore structure; i.e., there is incomplete wetting of the electrode surface. Saint et al. [30] observed similar results for an all-TFSI electrolyte The gradual fall in discharge capacity is possibly due to pore-blocking, which results from localized changes in lithium concentration (reflecting state-of-charge). As the concentration of lithium ions at the cathode surface rises (during charging), the chances increase that a phase with different properties will form within the porous region. For C_4mpyrTFSI–LiTFSI mixtures, Henderson and Passerini [31] have shown that the melting point increases significantly with the mole fraction of lithium ion in this region of the phase diagram [31]. Consequently, the loss of capacity may be indicative of the blockage of pores through deposition of a relatively lithium-rich phase.

Extended cycling of Li–$LiFePO_4$ (C_3mpyrFSI, 0.5 mol kg^{-1} LiTFSI) cells at 50 °C for in excess of 400 cycles shows a relatively constant charging efficiency (~100%). Ultimately, these cells fail due to the growth of dendritic forms of metallic lithium which eventually penetrate the separator and touch the cathode to cause a short circuit. Confirmation was obtained by disassembling cells that had completed prescribed service, in an argon-filled glove-box. Lithium anodes show roughened morphology, while separators display dark areas where the porous membrane has admitted in-growth by lithium. By comparison, the cathode coatings are, without exception, found to be in excellent condition, with no signs of spalling of cathode material or any obvious indication of a change in composition.

To examine further the phase purity of the $LiFePO_4$ after cycling, selected cathodes were subjected to XRD phase analysis at the end of the 50th discharge (state-of-charge = 0%). In Fig. 6(a) a control (uncycled) sample is compared with the cathodes from two cycled (50 cycles) cells: EC:DMC ($LiPF_6$) electrolyte (Fig. 6(b)) and C_3mpyrFSI (Fig. 6(c)). The large peak close to $2\theta = 21.5^\circ$ is due to the plastic film which was used to prevent exposure to atmosphere. There is no evidence in these data of phases other than $LiFePO_4$, which indicates that there has been no significant structural breakdown during cycling.

To obtain more information on the utility of a Li–$LiFePO_4$ cell with the C_3mpyrFSI–LiTFSI electrolyte solution, the discharge capacity was recorded at rates between C/10 and 4C, with a con-

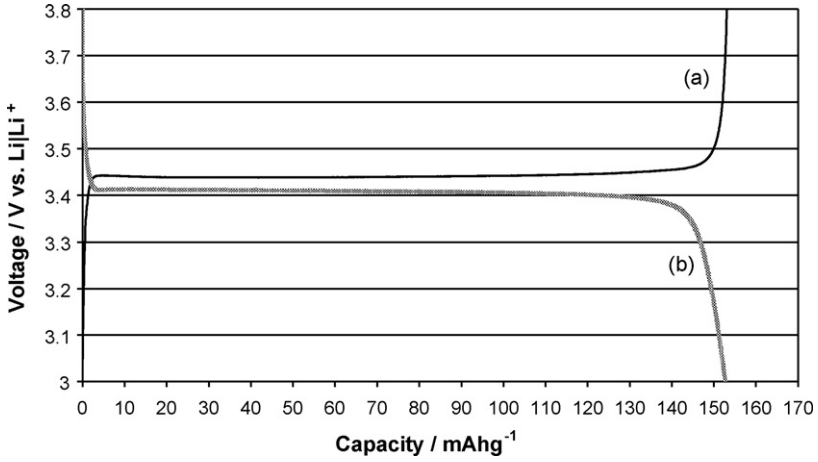

Fig. 4. Typical voltage–capacity plots for (a) charging; and (b) discharging of Li| C_3mpyrFSI–LiTFSI (0.5 mol kg^{-1}) |$LiFePO_4$ cell at C/10 charge–discharge rate (at 50 °C).

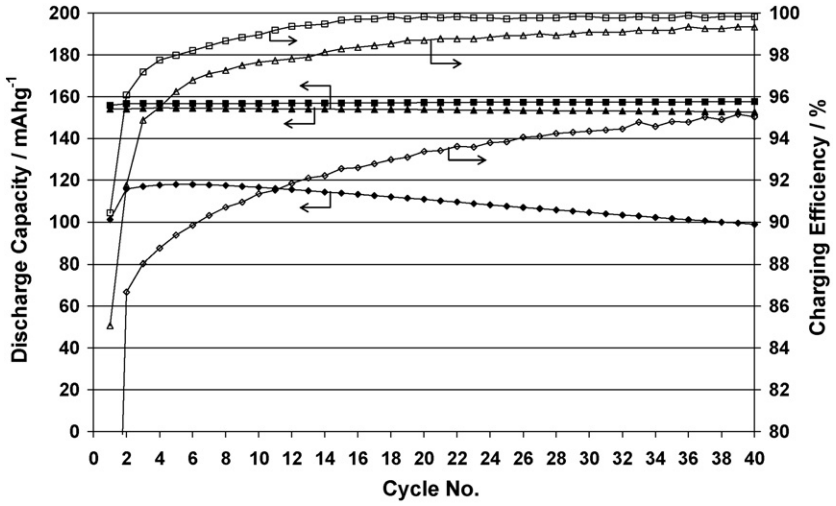

Fig. 5. Cycling performance (C/10 charge and discharge) at 50 °C of Li|electrolyte|$LiFePO_4$ cells with electrolytes solutions: (a) C_3mpyrFSI–LiTFSI (0.5 mol kg^{-1}) (square); (b) EC:DMC (1 M $LiPF_6$) (triangle); (c) C_4mpyrTFSI–LiTFSI (0.5 mol kg^{-1}) (diamond). Filled symbols—discharge capacity; open symbols—charging efficiency.

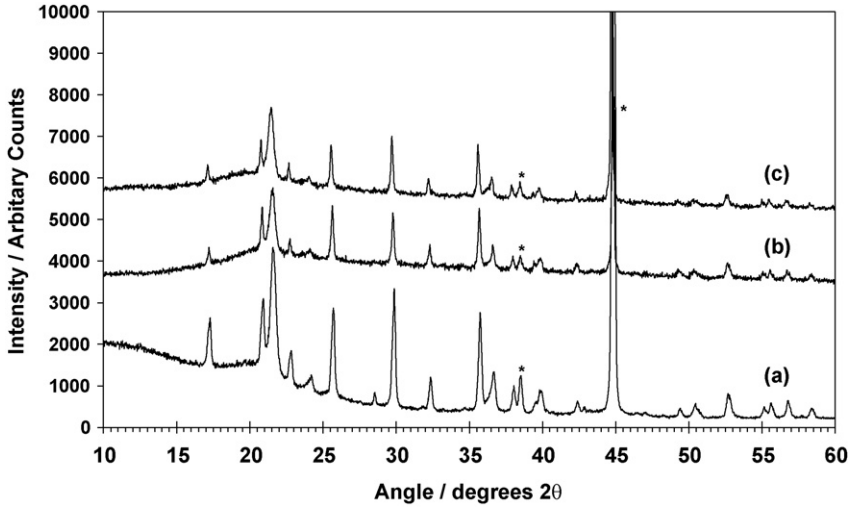

Fig. 6. X-ray powder diffraction pattern of $LiFePO_4$ cathode: (a) uncycled (control); (b) cycled in EC:DMC (1 M $LiPF_6$); (c) cycled in C_3mpyrFSI–LiTFSI (0.5 mol kg^{-1}). *Indicates aluminium peaks from foil.

stant C/10 charging rate (Fig. 7). Discharge capacities are collected in Table 1. Varying the discharge rate up to 4C, going through a sequence of multiple low- and high-rate discharge cycles, produces no permanent loss of discharge capacity at a given rate. Further, it is seen that even after a second sequence of varying discharge rates (Fig. 7(b)), the cell continues to deliver close to the original C/2 capacity after 250 cycles. This is further confirmation of the excellent cycling capability of the system. As anticipated though, the capacity does drop as the specific discharge rate increases, particularly when comparing the C/2 and 4C portions of the data. The overall charge/discharge capacity ratio (a measure of coulombic efficiency) is close to unity[1] throughout the whole range of discharge rates, so that the fall in capacity, especially at the higher discharge rates, is not the result of damage but rather it reflects the lithium transport limitations in the $LiFePO_4$ electrode. The inhibited lithium transport, which is inherently due to low electronic conductivity of this material, makes lithium intercalation in this case more difficult, especially with the larger crystallites and at higher discharge rates. Improving rate performance of this material would require the particle size to be reduced in order for electrolyte and conductive carbon to be in intimate contact with $LiFePO_4$ whilst reducing the lithium diffusion length.

Table 1
Discharge capacities at various rates (C/10 charge rate) of 1.8 mg cm^{-2} $LiFePO_4$ cathode in C_3mpyrFSI + 0.5 mol kg^{-1} LiTFSI at 50 °C.

Discharge rate	Discharge capacity (mAh g^{-1})
C/10	153
C/5	150
C/2	144
1C	137
2C	131
4C	110

In recent years, a small number of publications have demonstrated the use of RTIL-based electrolyte solutions with $LiFePO_4$ cathodes. Fernicola et al. [23] utilised TFSI variants of several pyrrolidinium RTILs and achieved ~105 and ~60 mAh g^{-1} at C/5 and 1C discharge rates, respectively (at room temperature). Shin et al. [3] utilised a blend of a polymer with the same pyrrolidinium ana-

[1] Departures from unity occur, as expected, on the first cycle after a change of discharge rate.

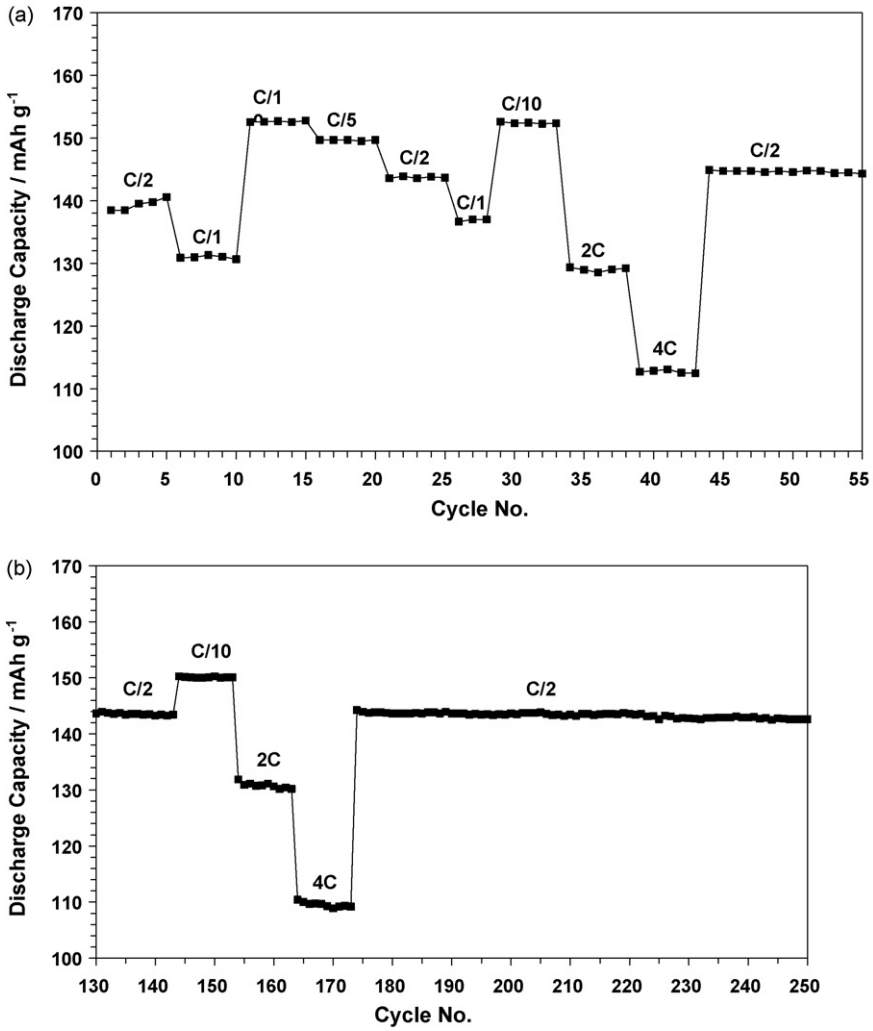

Fig. 7. Cycling performance of Li| C_3mpyrFSI–LiTFSI (0.5 mol kg^{-1}) |$LiFePO_4$ cell at indicated discharge rates (at 50 °C) for: (a) cycles 1–55; (b) cycles 130–250. Charging rate is constant at C/10.

logue and achieved a much higher capacity of ~150 mAh g^{-1} at the C/10 discharge rate (at 40 °C). In both of these cases, capacity fade was observed and was attributed to the electrolyte since coulombic efficiency was close to unity throughout cycling. More recently, Guerfi et al. [2] used a pyrrolidinium FSI RTIL in cells with a graphite anode, and observed a reversible capacity of ~150 mAh g^{-1} at 60 °C with negligible capacity fade. In the present study, similar capacities to that reported by other workers have been achieved but the results show clearly that pyrrolidinium FSI RTIL-based electrolyte solutions offer the distinct advantage of negligible capacity fade over a typical cycle-life of several hundred cycles at high efficiency. To the best of the authors knowledge, this is the first report that demonstrates the excellent combination of rate performance and cycle-life that can be achieved with a $LiFePO_4$ cathode, a metallic lithium anode and a C_3mpyrFSI RTIL-based electrolyte solution.

4. Summary and conclusions

It has been shown that RTILs from the grouping of pyrrolidinium sulfonylimides are suitable for use in a cell containing a lithium metal anode and a $LiFePO_4$ cathode. In particular, the combination of C_3mpyrFSI + 0.5 mol kg^{-1} LiTFSI has been shown to work effectively as an electrolyte solution with a metallic lithium anode where carbonate electrolytes are not suited. Excellent cycle-ability of the $LiFePO_4$ is obtained even when the cell is taken to a 4C discharge rate, at which the available discharge capacity is still 110 mAh g^{-1}, i.e., 72% of the C/10 value. Slightly lower capacities in C_3mpyrFSI RTIL are obtained at room temperature. These findings suggest that the kinetics of lithium diffusion in both $LiFePO_4$ and the RTIL are enhanced at the higher temperature. Further increases in capacity should be achievable, even with increased loading of cathode material, if the $LiFePO_4$ particle size is decreased, in order to overcome lithium diffusion limits.

Acknowledgements

This work was supported by CSIRO Energy Transformed Flagship and CSIRO Energy Technology, whom APL thanks for the provision of a postgraduate study award. The authors also gratefully acknowledge Ms Nicki Agron-Olshina (CSIRO Minerals) for assistance in the acquisition of XRD data.

References

[1] K. Ozawa, Solid State Ionics 69 (1994) 212–221.
[2] A. Guerfi, S. Duchesne, Y. Kobayashi, A. Vijh, K. Zaghib, J. Power Sources 175 (2008) 866–873.
[3] J.H. Shin, W.A. Henderson, S. Scaccia, P.P. Prosini, S. Passerini, J. Power Sources 156 (2006) 560–566.
[4] S. Seki, Y. Kobayashi, H. Miyashiro, Y. Ohno, A. Usami, Y. Mita, M. Watanabe, N. Terada, Chem. Commun. (2006) 544–545.

[5] A.K. Padhi, K.S. Nanjundaswamy, J.B. Goodenough, J. Electrochem. Soc. 144 (1997) 1188–1194.
[6] A. Yamada, S.C. Chung, K. Hinokuma, J. Electrochem. Soc. 148 (2001) A224–A229.
[7] Y.W. Denis, C. Fietzek, W. Weydanz, K. Donoue, T. Inoue, H. Kurokawa, S. Fujitani, J. Electrochem. Soc. 154 (2007) A253–A257.
[8] N.J. Iltchev, Y. Chen, S. Okada, J.-I. Yamaki, J. Power Sources 119 (2003) 749–754.
[9] D. Wang, H. Li, S. Shi, X. Huang, L. Chen, Electrochim. Acta 50 (2005) 2955–2958.
[10] S. Seki, Y. Mita, H. Tokuda, Y. Ohno, Y. Kobayashi, A. Usami, M. Watanabe, N. Terada, H. Miyashiro, Electrochem. Solid State Lett. 10 (2007) A237–A240.
[11] L.F. Nazar, O. Croznier, in: G.-A. Nazri, G. Pistoia (Eds.), Lithium Batteries: Science and Technology, Springer, New York, 2009.
[12] J.H. Shin, W.A. Henderson, S. Passerini, Electrochem. Commun. 5 (2003) 1016–1020.
[13] H. Sakaebe, H. Matsumoto, Electrochem. Commun. 5 (2003) 594–598.
[14] S. Seki, Y. Kobayashi, H. Miyashiro, Y. Ohno, A. Usami, Y. Mita, N. Kihira, M. Watanabe, N. Terada, J. Phys. Chem. B 110 (2006) 10228–10230.
[15] J. Xu, J. Yang, Y. NuLi, J. Wang, Z. Zhang, J. Power Sources 160 (2006) 621–626.
[16] J.H. Shin, P. Basak, J.B. Kerr, E.J. Cairns, Electrochim. Acta 54 (2008) 410–414.
[17] G.X. Wang, L. Yang, S.L. Bewlay, Y. Chen, H.K. Liu, J.H. Ahn, J. Power Sources 146 (2005) 521–524.
[18] S. Franger, F. Le Cras, C. Bourbon, H. Rouault, Electrochem. Solid State Lett. 5 (2002) A231–A233.
[19] D. Zane, M. Carewska, S. Scaccia, F. Cardellini, P.P. Prosini, Electrochim. Acta 49 (2004) 4259–4271.
[20] G. Meligrana, C. Gerbaldi, A. Tuel, S. Bodoardo, N. Penazzi, J. Power Sources 160 (2006) 516–522.
[21] P.C. Howlett, D.R. MacFarlane, A.F. Hollenkamp, Electrochem. Solid State Lett. 7 (2004) A97–A101.
[22] P.C. Howlett, N. Brack, A.F. Hollenkamp, M. Forsyth, D.R. MacFarlane, J. Electrochem. Soc. 153 (2006) A595–A606.
[23] A. Fernicola, F. Croce, B. Scrosati, T. Watanabe, H. Ohno, J. Power Sources 174 (2007) 342–438.
[24] H. Matsumoto, H. Sakaebe, K. Tatsumi, M. Kikuta, E. Ishoko, M. Kono, J. Power Sources 160 (2006) 1308–1313.
[25] S. Seki, Y. Ohno, Y. Kobayashi, H. Miyashiro, A. Usami, Y. Mita, H. Tokuda, M. Watanabe, K. Hayamizu, S. Tsuzuki, M. Hattori, N. Terada, J. Electrochem. Soc. 154 (2007) A173–A177.
[26] M. Holzapfel, C. Jost, P. Novak, Chem. Commun. (2004) 2098–2099.
[27] B. Zhao, Y. Jiang, H. Zhang, H. Tao, M. Zhong, Z. Jiao, J. Power Sources 189 (2009) 462–466.
[28] S. Franger, F. Le Cras, C. Bourbon, H. Rouault, J. Power Sources 119–121 (2003) 252–257.
[29] P.P. Prosini, D. Zane, M. Pasquali, Electrochim. Acta 46 (2001) 3517–3523.
[30] J. Saint, A.S. Best, A.F. Hollenkamp, J. Kerr, J.H. Shin, M.M. Doeff, J. Electrochem. Soc. 155 (2008) A172–A180.
[31] W.A. Henderson, S. Passerini, Chem. Mater. 16 (2004) 2881–2885.